GEOPHYSICS. VOL. 76, NO. 5 (SEPTEMBER-OCTOBER 2011); P. WB21–WB26, 12 FIGS.
10.1190/GEO2011-0043.1

Investigation of deep-water Gulf of Mexico subsalt imaging using anisotropic model, data set and RTM — Tempest

Fatmir Hoxha[1], Jacqueline O'Connor[1], Jeff Codd[1], David Kessler[1], Alex Bridge[2], Dana Jurick[2], Richard Brietzke[2], and Kenneth Beeney[2]

ABSTRACT

Performing accurate depth-imaging is an essential part of deep-water Gulf of Mexico exploration and development. Over the years, depth-imaging technology has provided reliable seismic images below complicated salt bodies, and has been implemented in workflows for both prospect generation as well as reservoir development. These workflows include time domain preprocessing using various multiple elimination techniques, anisotropic model building, and depth-imaging using anisotropic reverse time migration (RTM). However, the accuracy of the depth-migrated volumes is basically unknown because they are tested only in the locations where a well is drilled. In order to learn about the accuracy of anisotropic deep water Gulf of Mexico model building, and depth-imaging tools which are used for processing and imaging of field acquired data, we created a 3D vertical transverse isotropic (VTI) anisotropic earth model and a 3D seismic data set representing subsalt Gulf of Mexico geology. The model and data set are referred to as the Tempest data set, the original being created several years ago. The recent model and data set were created incorporating upgraded technology to reflect recent developments in data acquisition, model building and depth-imaging. Our paper presents the new Tempest anisotropic model, data set, and RTM prestack depth-migration (PSDM) results. The Tempest RTM PSDM is being used to learn about the differences between the exact geological model and the RTM PSDM image, helping in the interpretation of real RTM prestack depth-migrated data.

INTRODUCTION

The Tempest Project was initiated a few years ago in an effort to analyze the accuracy of depth-imaging technology applied in deep-water Gulf of Mexico. The initial project was executed in three phases. Phase one included the design and construction of a realistic deep-water Gulf of Mexico geological model, and the simulation and imaging of the data set using the known velocity model. In phase two of the project, the simulated data set was provided to several processing companies who regularly perform depth-imaging for Devon Energy. These processing companies constructed a velocity model and applied prestack depth-migration to the data with the derived model in the same manner as if the data were real Gulf of Mexico field data. The result of this step was a series of developed models. Phase three included the interpretation and analysis of the depth imaged volumes resulting from phase two with the objectives being to (1) compare the prestack depth-migration results obtained using the derived model to results achieved using the exact earth model, (2) compare the developed models to the exact model, and (3) compare the synthetic imaged data to field acquired data sets. The results of this study were described in Seitchik et al. (2009). In this paper, we describe the fourth phase of the Tempest project, which included upgrading the model to a VTI anisotropic model, simulating and recording an anisotropic synthetic data set using VTI forward modeling, and performing depth-imaging using VTI reverse time migration (RTM) prestack depth migration (PSDM).

Several new data acquisition, processing, and depth-imaging technologies have been introduced to the industry over the past

Manuscript received by the Editor 3 February 2011; revised manuscript received 21 June 2011; published online 21 November 2011.
[1]SeismicCity Corporation, Houston, Texas, USA. E-mail: dkessler@seismiccity.com; fhoxha@seismiccity.com; joconnor@seismiccity.com; jcodd@seismiccity.com.
[2]Devon Energy Corporation, Houston, Texas, USA. E-mail: alex.bridge@dvn.com; dana.jurick@dvn.com; richard.brietzke@dvn.com; kenneth.beeney@dvn.com.

few years. These include the recording of wide-azimuth marine data (Napier et al., 2010), the use of RTM (Baysal et al., 1983) as the leading tool for prestack depth-migration, a move from isotropic to anisotropic model building and depth-imaging (Bakulin et al., 2010), and the development and use of more sophisticated multiple elimination techniques (Dragoset et al., 2008). Today's processing of modern Gulf of Mexico seismic data uses mainly wide-azimuth data compared to processing of narrow-azimuth data in the past. The main process applied in time domain preprocessing is surface related multiple elimination using new techniques as shown in Dragoset et al. (2008). Following with model building, today's multiparameter anisotropic models replace the older velocity models. This requires the development of new techniques and workflows for construction of an anisotropic earth model. Finally, using the great advances in computer technology, the more computationally intensive 3D anisotropic common-shot RTM became the prestack depth-migration algorithm which is most commonly used for application of depth-imaging. Utilizing lessons learned from the first Tempest Project, the model, data set, and prestack depth-migration were upgraded so that they can be used in the testing, evaluation, and assessment of these new technologies.

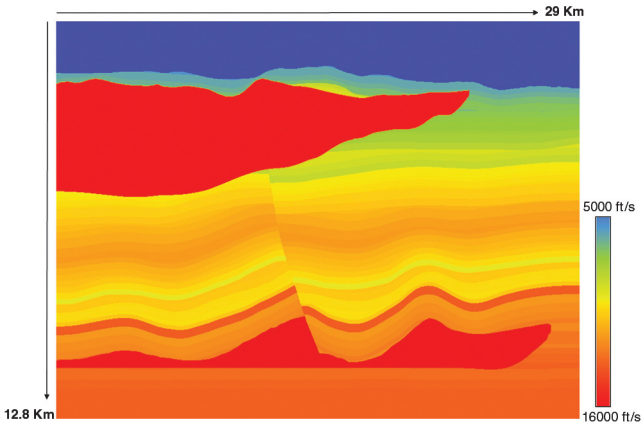

Figure 1. A velocity inline display from the Tempest anisotropic model.

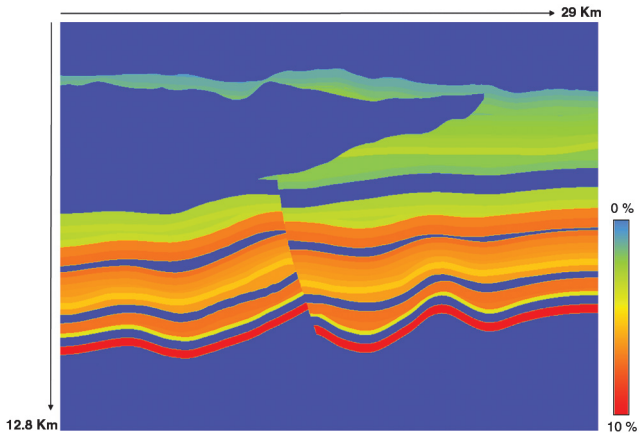

Figure 2. A delta inline display from the Tempest anisotropic model.

THE TEMPEST MODEL

In the latest iteration, the Tempest model was updated to a complete VTI anisotropic model consisting of a vertical velocity field, as well as delta and epsilon fields. The model was constructed using actual well data and is a calibrated representation of the deep-water Gulf of Mexico exploration setting which involves complex salt bodies and clastic stratigraphy. Major structural features are the same as in the original Tempest model and include varying water bottom geometry, allochthonous, and autochthonous salt bodies including salt roots, allochthonous minibasins, subsalt faulting, and subsalt three-way and four-way target structures (Kessler et al., 2008). The structural geometries and distribution of the salt-related features are accurately represented following documented subsalt features observed in the deep-water Gulf of Mexico.

The Tempest anisotropic model was built in two steps. First, the structural framework was constructed using major Gulf of Mexico structural features as mentioned above. Second, several deep-water Gulf of Mexico well logs were used for the construction of a velocity and anisotropic (i.e., epsilon and delta) functions for creation of a 3D VTI anisotropic earth model (Walsh et al., 2007). Blocked versions of the well logs were used to populate the structural model, resulting in a detailed geological model.

The Tempest anisotropic model consists of three model parameters; vertical velocity, delta field, and epsilon field, with epsilon values equal to twice the delta values. The three-parameter anisotropic model enabled the simulation and imaging of the Tempest data using wave propagation equations which are used in the industry for application of anisotropic RTM. The Tempest model is 957^2 in size with a maximum depth of 12.8 km. It consists of about 40 layers with an average layer thickness of 200 m, and represents a detailed VTI anisotropic geological model for deep-water Gulf of Mexico (Figures 1 and 2).

NUMERICAL SIMULATION

Using the new Tempest model, a synthetic data set was created to be used for (1) testing of wide-azimuth data processing such as 3D surface related multiple elimination (Dragoset et al., 2008) (2) testing of anisotropic model building techniques (Bakulin et al., 2010), and (3) testing of new depth-imaging techniques such as 3D anisotropic RTM.

VTI anisotropic acoustic wavefield simulation was used to incorporate VTI anisotropy in the data set (Zhang, and Zhang, 2009). The forward modeling for the VTI media (equation 1) is viewed as the propagation of two quantities, p and q, where p is the "acoustic" wavefield and q is an auxiliary variable dependent on p and used to simplify the solution of the partial differential equations used for wave propagation. A high-order spatial finite-differences operator (eighth-order) was used in the forward modeling. A 20 m grid sampling in both the X and Y directions and 18.3 m grid sampling in the Z direction were selected for the simulation to achieve wave propagation with minimal numerical dispersion for the 0–25 Hz frequency bandwidth that was used in the simulation. For absorption of reflections from the sides of the model, tapered boundaries were added (Cerjan et al., 1985). The following is the wave equation approximation used for the simulation of the VTI anisotropic data set:

$$\left[2(\varepsilon-\delta)\left(\frac{\partial^2}{\partial x^2}+\frac{\partial^2}{\partial y^2}\right)(p+q)\right]=\frac{1}{v^2}\frac{\partial^2}{\partial t^2}q$$
$$\left[(1+2\delta)\left(\frac{\partial^2}{\partial x^2}+\frac{\partial^2}{\partial y^2}\right)(p+q)+\frac{\partial^2}{\partial z^2}p\right]=\frac{1}{v^2}\frac{\partial^2}{\partial t^2}p \qquad (1)$$

In order to use the data set for investigating wide-azimuth acquisition designs, each shot was recorded over a large areal extent. This was achieved by recording 100 lines of 400 channels for each simulated shot. The line spacing that was used is 80 m and the receiver spacing is 40 m. A total of 55 sail lines were simulated with shot spacing of 80 m and boat array pass distance of 500 m. This geometry resulted in a uniform fold and offset/azimuth distributions shown in (Figure 3). The recording of large shot patches enabled us to extract subsets from the full data set to test the effects of sampling decimation on processing and imaging. Using a subset of the recorded data set as input to anisotropic Kirchhoff summation PSDM shown in (Figures 4 and 5), we verified that the use of a larger recording patch results in better sampling which in turn, leads to better elimination of multiple energy. Application of depth-imaging techniques using subsets of the input data can be used for investigation of various acquisition scenarios.

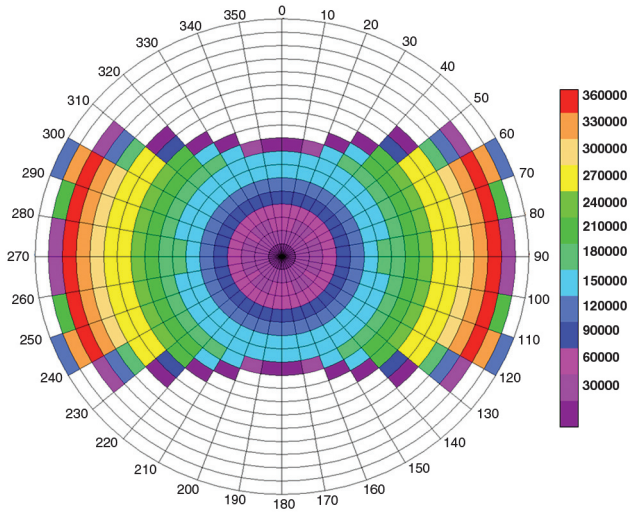

Figure 3. Offset/azimuth plot generated from the wide-azimuth Tempest data set. The cable length is 8 km and the crossline distance is 4 km. The selected acquisition parameters resulted with a uniform fold of 400.

In order to generate a data set that can be used for testing of new developments in both processing and imaging, free surface boundary conditions were used. The resulting data set includes both inner bed as well as surface related multiples. The source input wavelet used in the simulation was a 25 Hz broadband Butterworth wavelet. Using the numerical scheme discussed above, 20,075 shots were generated where each shot is recorded over a 16×8 Km area consisting of 40,000 recorded channels. The recording time used was 14 seconds. The resulting data set is 6TB in size and is stored in the SEG standard format (SEGY). In order to be able to generate a synthetic data set of this size in a reasonable time frame, a hybrid CPU/GPU computer cluster was used for the numerical simulation (Foltinek et al., 2009).

DEPTH-IMAGING

One of the main developments in the past few years in the area of depth-imaging is the routine use of 3D common-shot RTM as the leading algorithm for imaging of both marine and land seismic data (Fletcher et al., 2005). RTM was introduced about 30 years ago as a 2D poststack depth-migration algorithm (McMechan, 1982; Loewenthal and Mufti, 1983). For many years, RTM was not used in a production environment due to its high computational demands, which could not be met by the computer technology of the time. Advancements over the past few years in computational power, as well as computer storage capacity and computer network connection speed, have enabled the implementation of 3D RTM in the industry. Following the basic concept introduced by Baysal et al.

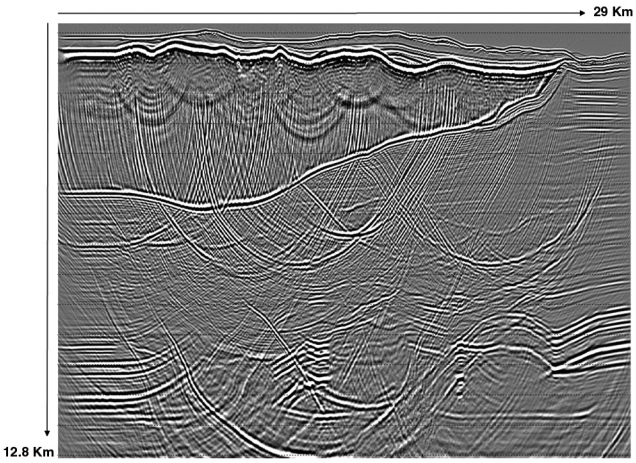

Figure 4. Depth-migrated section resulting from inputting of a 400 m crossline tile subset of the data. This is equivalent to a single boat acquisition using eight streamers on each side with 100 m streamer separation. PSDM is done using an anisotropic Kirchhoff summation algorithm. The multiples migrated at the subsalt section are a result of both surface related as well as inner bed multiples.

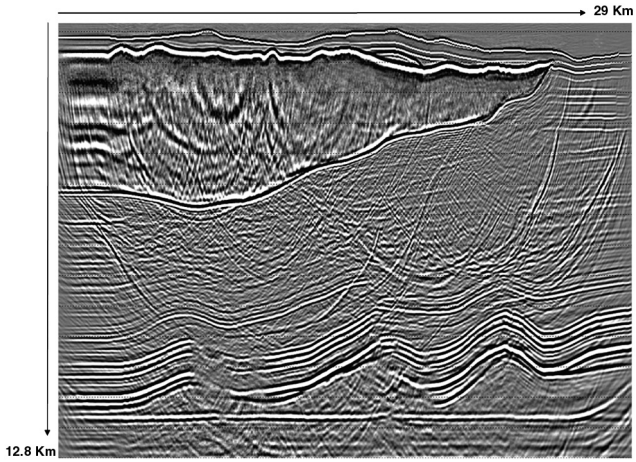

Figure 5. Depth-migrated section resulting from inputting 4 km crossline tile subset of the data. PSDM is done using an anisotropic Kirchhoff summation algorithm. Compared to the section showed in Figure 4, multiple energy is reduced due to the better sampling of multiples. The deeper salt is now well imaged, compared to the image show in Figure 4.

(1983), RTM has now been implemented and used in production processing for 3D common-shot migration in isotropic, as well as VTI and TTI anisotropic media (Duveneck et. al, 2008, Zhang and Zhang, 2008).

VTI anisotropic common-shot RTM is the algorithm that was used for depth-imaging of the VTI anisotropic Tempest data set. Figures 6 and 7 show the imaging results in the vicinity of the subsalt fault and subsalt vertical salt stalk, respectively. Clear imaging of subsalt faults is quite difficult to obtain using older Kirchhoff summation PSDM, or even one way downward propagation wave equation PSDM. Using RTM and a very accurate velocity model, subsalt faults can be better imaged and interpreted with much more confidence. Imaging of steep salt stalks connecting the autochthonous salt to the allochtonous salt is very difficult, even when using RTM prestack depth-migration. Because we know the actual size of the salt stalk in the Tempest data set and model we are able to measure the area of low illumination around the vertical salt stalk. That helps in the interpretation of the true size of the salt stalk when using real field data. Figure 8 shows a depth slice from the anisotropic wide-azimuth RTM PSDM at the subsalt section. Both the subsalt four-way and the subsalt three-way closure at the fault are well imaged. The low illumination area around the vertical subsalt salt stalk is greatly reduced compared to imaging results obtained using narrow-azimuth isotropic data. The same set of numerical equations that were used for the generation of the Tempest synthetic data set were used as the basis for the RTM algorithm. Because the depth-imaging of the Tempest data set was performed on synthetic data that had no preprocessing or prior multiple elimination, we were able to learn about the elimination of multiple energy using imaging and stacking of the wide-azimuth data set. Migrating the data set using the exact model and a two-way wave equation PSDM, imaging of multiple energy was reduced by better stacking of primary reflections. Further improvement can be made to the Tempest PSDM image by applying preprocessing for elimination of free surface multiples. The superior imaging of wide-azimuth data using RTM algorithm over imaging of isotropic narrow-azimuth data using Kirchhoff summation algorithm is shown in (Figures 9, 10, 11, and 12). Figure 10 shows that by using a two-way wave equation PSDM algorithm (i.e., RTM), we can eliminate artifacts produced when using Kirchhoff summation algorithm for imaging around vertical salt stalks and below complex top salt as shown in (Figure 9). Figure 12 shows that a subsalt fault can be imaged using the wide-azimuth RTM PSDM algorithm when compared to

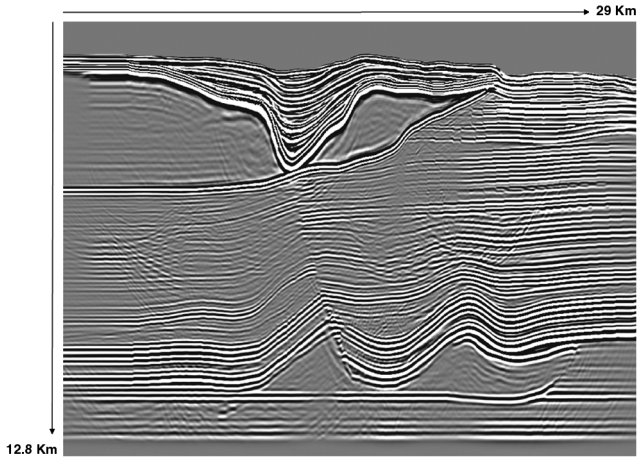

Figure 6. A vertical section display from the Tempest anisotropic RTM volume. This section shows the imaging at the subsalt fault area. The subsalt fault is clearly imaged. However, even when using the exact velocity model, some of the reflections of the sedimentary layers from the two sides of the fault might leak to the other side of the fault. This observation can help in the interpretation of real data subsalt faults. The artifacts evident in the sedimentary section are free surface and inner bed multiples that did not stack out during PSDM.

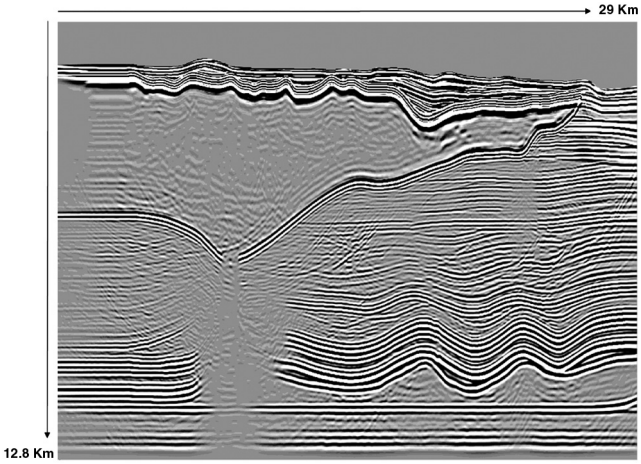

Figure 7. RTM PSDM image of the seismic data at the area of the narrow salt stalk. From this result we can quantitatively measure the area of low illumination around the salt stalk. We can use the relation between the real size of the salt stalk and its seismic signature to assist in interpretation of real data subsalt stalks. The vertical subsalt stalk is not imaged since reflections from this part of the salt were not recorded on the surface using the wide-azimuth acquisition geometry that was used in this study.

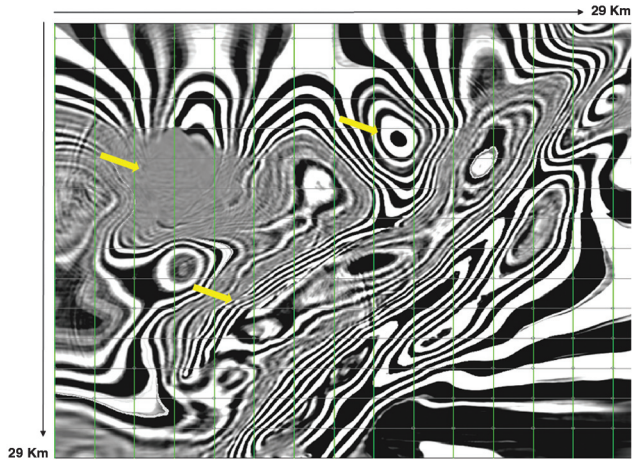

Figure 8. RTM PSDM depth slice showing the three Tempest subsalt exploration targets; a four-way closure, a three-way closure against the subsalt fault, and the subsalt sedimentary truncations against the salt stalk. These typical subsalt exploration targets are commonly interpreted using real depth-migrated data. Having the Tempest image can help us in understanding the seismic signature of these subsalt features.

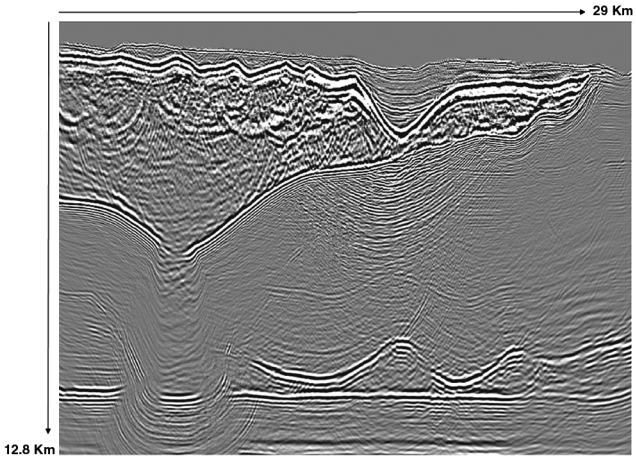

Figure 9. Kirchhoff summation PSDM image of the Tempest data at the area of the narrow salt stalk generated from the first Tempest isotropic narrow-azimuth data set.

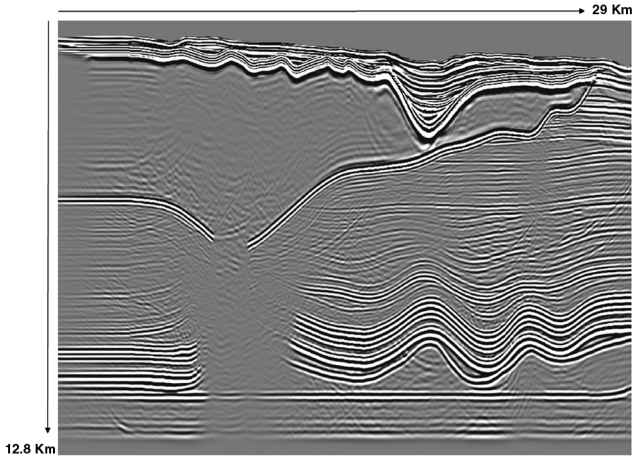

Figure 10. RTM PSDM image of the Tempest data at the area of the narrow salt stalk generated from the anisotropic wide-azimuth Tempest data set.

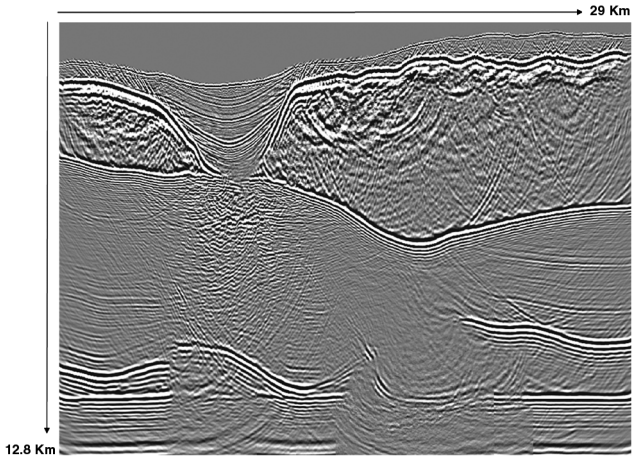

Figure 11. Kirchhoff summation PSDM image of the Tempest data at the basin area and the subsalt fault generated from the first Tempest isotropic narrow-azimuth data set.

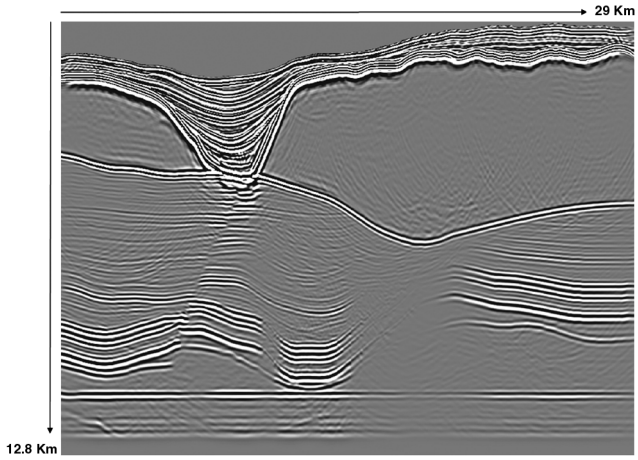

Figure 12. RTM PSDM image of the Tempest data at the basin area and the subsalt fault generated from the wide-azimuth anisotropic Tempest data set.

Kirchhoff summation PSDM of the narrow-azimuth data shown in (Figure 11). The above depth-imaging comparisons are produced using the exact velocity model. Because the RTM PSDM algorithm can image subsalt geology so well, we conclude that the focus of development of new depth-imaging technology should be shifted to the construction of more accurate velocity models when using real field data.

CONCLUSIONS

The objective of our study was to generate a realistic model and synthetic anisotropic data set. Having a known velocity model, we can quantitatively measure the accuracy of the anisotropic model building and depth-imaging techniques that are routinely performed using actual field data (Brietzke et al., 2008), as well as test new depth-imaging workflows applied for subsalt exploration in the deep-water Gulf of Mexico. These workflows include new techniques for time domain multiple removal, construction of anisotropic depth models, and application of anisotropic RTM as the leading prestack depth-migration algorithm, as well as interpretation and construction of subsalt structural maps used for locating new subsalt exploration wells. Utilizing VTI PSDM RTM to image the wide-azimuth anisotropic Tempest data set clearly demonstrates the advancement in depth-imaging resulting from new data acquisition techniques and prestack depth-migration algorithms that have been implemented during the past few years. Having better seismic data (wide-azimuth data rather than narrow-azimuth data) and the use of more advanced depth-imaging algorithms (RTM instead of Kirchhoff summation algorithm) shifts the focus in the development of depth-imaging technology to model building techniques. Advancements in model building can be further investigated and tested using a simulated data set such as the Tempest data set. The use of a full 3D synthetic anisotropic data set for testing new acquisition and depth-imaging technologies will lead to a better understanding of the advantages and shortcomings of these modern processing techniques while providing key insights into the accuracy, resolution, and limitations of the anisotropic models that we currently construct when using field acquired wide-azimuth seismic data. There are several public synthetic data sets which are available

for the industry and academia. The Tempest data set is unique as it is a 3D anisotropic data set which is based on true deep-water Gulf of Mexico geology and can be available for use by the industry and academia. We expect that, in the future, more 3D data sets like this will be produced as new processing and imaging technologies require more complex models for verification purposes.

ACKNOWLEDGMENTS

The original Tempest data was provided courtesy of Devon Energy Corporation. We would like to thank the reviewers of the paper for their help in improving the text and helping in making the presentation of our work more general.

REFERENCES

Bakulin, A., Y. Liu, O. Zdraveva, and K. Lynos, 2010, Anisotropic model building with wells and horizons: Gulf of Mexico case study comparing different approaches: The Leading Edge, 1450–1460.

Baysal, E., D. Kosloff, and J. W. C. Sherwood, 1983, Reverse time migration: Geophysics, **48**, 1514–1524, doi:10.1190/1.1441434.

Brietzke, R., A. Bridge, D. Jurick, and A. Seistchik, 2008, Evaluating the accuracy of deep-water Gulf of Mexico depth-imaging — the Tempest results: 78th Annual International Meeting, SEG, Expanded Abstracts, **27**, 383–387.

Cerjan, C., D. Kosloff, R. Kosloff, and M. Reshef, 1985, A nonreflecting boundary condition for discrete acoustic and elastic wave equations: Geophysics, **50**, 1266–1272,doi: 10.1190/1.1441945.

Dragoset, B., I. Moore, M. Yu, and W. Zhao, 2008, 3D general surface multiple prediction: An algorithm for all surveys: 78th Annual International Meeting, SEG, Expanded Abstracts, 2426–2430.

Duveneck, E., P. Milcik, P. M. Bakker, and C. Perkins, 2008, Acoustic VTI wave equations and their application for anisotropic reverse-time migration: 78th Annual International Meeting, SEG, Expanded Abstracts, **27**, 2186–2190.

Fletcher, F. R., P. Fowler, P. Kitchenside, and U. Albertin, 2005, Suppressing artifacts in prestack reverse time migration: 75th Annual International Meeting, SEG, Expanded Abstracts, **24**, 2049–2051.

Foltinek, D., D. Eaton, J. Mahovsky, P. Moghaddam, and R. McGarry, 2009, Industrial-scale reverse time migration on GPU hardware: 79th Annual International Meeting, SEG, Expanded Abstracts, **28**, 2789-2793.

Kessler, D., J. Codd, F. Hoxha, C. Pignol, A. Bridge, R. Brietzke, A. Seitchik, and D. Jurick, 2008, A realistic deep-water Gulf of Mexico 3D simulation and imaging — The Tempest simulation, data set and imaging: 78th Annual International Meeting, SEG, Expanded Abstracts, **27**, 378–382.

Loewenthal, D. I., and I. R. Mufti, 1983, Reversed time migration in spatial frequency domain: Geophysics, **48**, 627–635, doi: 10.1190/1.1441493.

McMechan, G. A., 1982, Determination of source parameters by wavefield extrapolation: Geophysical Journal of the Royal Astronomical Society, **71**, 613–628.

Napier, P., I. M. Threadgold, P. G. Aas, and D. J. Harrison, 2010, Worldwide WATS: Optimising both the cost and data quality: 80th Annual International Meeting, SEG, Expanded Abstracts, **29**, 6–10.

Seitchick, A., D. Jurick, A. Bridge, R. Brietzke, K. Beeney, J. Codd, F. Hoxha, C. Pignol, and D. Kessler, 2009, The tempest project — Addressing challenges in deep-water Gulf of Mexico depth-imaging through geologic models and numerical: The Leading Edge, 546–553.

Walsh, J., B. Sinha, T. Plona, D. Miller, D. Bentley, and M. Ammermann, 2007, Derivation of anisotropy parameters in a shale using borehole sonic data: 77th Annual International Meeting, SEG, Expanded Abstracts, **26**, 323–327.

Zhang, H., and Y. Zhang, 2008, Reverse time migration in 3D heterogeneous TTI media: 78th Annual International Meeting, SEG, Expanded Abstracts, **27**, 2196–2200.

Zhang, Y., and H. Zhang, 2009, A stable TTI reverse time migration and its implementation: 79th Annual International Meeting, SEG, Expanded Abstracts, 2794–2798.

Zhou, H., G. Zhang, and B. Bloor, 2006, Anisotropic acoustic wave equation for VTI media: Presented at the 68th Annual International Conference an Exhibition, EAGE.